

ζ_e/x are obtained for $T_m^\circ = 69^\circ\text{C}$, the latter being invariant with molecular weight. Although this type of analysis cannot be used to directly determine a value for T_m° , an erroneous choice of T_m° leads to clearly suspect results.

In summary, we have reemphasized the need to distinguish between two situations in analyzing the equilibrium melting of chain molecules. One is based on the melting of oligomers, as, for example, *n*-alkanes, which require that molecular crystals be formed. This analysis can lead to the equilibrium melting temperature, T_m° , of an infinitely long chain. The Flory-Vrij result has been shown to be the correct one for this case. On the other hand, real polymer chains of finite length, no matter how well fractionated, cannot form molecular crystals. Hence, although they have the same value for T_m° , they must be analyzed differently. A quite different melting temperature-molecular weight relation results. Because the parameters involved here are also molecular weight dependent, it is not possible to correctly extrapolate to T_m° using solely the melting temperatures of equilibrium crystallites formed by chains of finite length.

Acknowledgment. Support of this work by Exxon Chemical Corp. is gratefully acknowledged.

Registry No. Polyethylene (homopolymer), 9002-88-4; poly(ethylene glycol) (SRU), 25322-68-3.

References and Notes

- (1) Mandelkern, L. "Crystallization of Polymers"; McGraw-Hill: New York, 1964.
- (2) Mandelkern, L.; Stack, G. M.; Mathieu, M. In *Anal. Calorim.*, in press.
- (3) Stack, G. M. Ph.D. Dissertation, Florida State University, 1983.
- (4) Flory, P. J. *J. Chem. Phys.* **1949**, *17*, 223.
- (5) Flory, P. J.; Vrij, A. *J. Am. Chem. Soc.* **1963**, *85*, 3548.
- (6) Wunderlich, B.; Czornyj, G. *Macromolecules* **1977**, *10*, 960.
- (7) Buckley, C. P.; Kovacs, A. J. *Prog. Colloid Polym. Sci.* **1975**, *58*, 44.
- (8) Hay, J. N. *J. Polym. Sci., Polym. Chem. Ed.* **1976**, *14*, 2845.
- (9) Fatou, J. G.; Mandelkern, L. *J. Phys. Chem.* **1965**, *69*, 417.
- (10) Quinn, F. A. Jr.; Mandelkern, L. *J. Am. Chem. Soc.* **1958**, *80*, 3178.
- (11) Finke, H. L.; Gross, M. E.; Waddington, G.; Huffman, H. M. *J. Chem. Soc.* **1954**, *76*, 33.
- (12) Broadhurst, N. G. *J. Chem. Phys.* **1962**, *36*, 2578.
- (13) Hay, J. N. *J. Polym. Sci., Polym. Lett. Ed.* **1970**, *8*, 395.
- (14) Schaerer, A. A.; Busso, C. J.; Smith, A. F.; Skinner, L. *J. Am. Chem. Soc.* **1955**, *77*, 2017. (a) Mazee, W. M. *Recl. Trav. Chim. Pays-Bas* **1948**, *67*, 197.
- (15) Mandelkern, L. In "Progress in Polymer Science"; Jenkins, A. D., Ed.; Pergamon Press: New York, 1970.
- (16) Atkinson, C. M. L.; Richardson, M. J. *Trans. Faraday Soc.* **1969**, *65*, 749.
- (17) Heitz, W.; Wirth, T.; Peters, R.; Strobl, G.; Fischer, E. W. *Makromol. Chem.* **1972**, *162*, 63.
- (18) Mandelkern, L.; Price, J. M.; Gopalan, M.; Fatou, J. G. *J. Polym. Sci., Part A-2* **1966**, *4*, 385.
- (19) Varnell, W. D.; Harrison, J. R.; Wang, J. I. *J. Polym. Sci., Polym. Phys. Ed.* **1980**, *19*, 1577.
- (20) Runt, J.; Harrison, I. R.; Dobson, S. J. *Macromol. Sci., Phys.* **1980**, *B17*, 99.
- (21) Beech, D. R.; Booth, C. J. *J. Polym. Sci., Part B* **1970**, *8*, 731.
- (22) Allen, R. C. M.S. Thesis, Florida State University, 1980.
- (23) Hay, J. N. *J. Chem. Soc., Faraday Trans.* **1972**, *68*, 656.
- (24) Stack, G. M.; Voigt-Martin, I. G.; Mandelkern, L. *Macromolecules*, in press.
- (25) We thank Professor G. Strobl for furnishing us with these samples. We also note that in their work the study of the thermodynamics of fusion was not of primary concern.
- (26) It must be recognized that the molecular weight range over which extended-chain crystals are formed is severely limited.²⁴

Regime III Crystallization in Polypropylene^{†,‡}

Elizabeth J. Clark

Center for Building Technology, National Bureau of Standards, Washington, D.C. 20234

John D. Hoffman*

Engineering Materials Program, Department of Chemical and Nuclear Engineering, University of Maryland, College Park, Maryland 20742. Received November 15, 1983

ABSTRACT: The recently developed theory for regime III crystallization from the melt is applied to isotactic polypropylene (i-PP) spherulite growth rate data. As the temperature decreases, a marked upward change in the slope of the published growth rate vs. temperature curves is observed, which is interpreted as a regime II \rightarrow regime III transition. (A regime I \rightarrow regime II transition would have exhibited a downward change in slope with decreasing temperature.) The regime II \rightarrow regime III transition occurs near 137°C , which corresponds to an undercooling of $\Delta T \sim 48^\circ\text{C}$. The experimentally observed change of slope in plots of $\ln G + U^*/R(T - T_\infty)$ vs. $1/T(\Delta T)$ at the II \rightarrow III transition is 2.087, which is close to the theoretically predicted value of 2. Also, the ratio of the preexponential factors for regimes III and II, $G_{0(\text{III})}/G_{0(\text{II})}$, is reasonably close to the theoretical estimate. Nucleation constants for i-PP are determined, and the surface free energies of $q \approx 11.5$ erg cm^{-2} and $\sigma_e \approx 65$ – 70 erg cm^{-2} are estimated. The latter leads to a work of chain folding of $q \approx 6.4$ – 6.8 kcal mol^{-1} , applicable to both regimes II and III. The q values are physically reasonable and fit into a more general picture for hydrocarbon polymers with $-\text{C}-\text{C}-$ backbones. A method of obtaining q directly from the observed growth rate data without knowing the enthalpy of fusion is illustrated. Growth rate data on syndiotactic polypropylene are discussed briefly. The significance of regime III crystallization is discussed in a general way.

Introduction

At a moderately large undercooling, isotactic polypropylene (i-PP) exhibits a distinct and rather abrupt upward trend in its spherulite growth rate vs. temperature

curve as the crystallization temperature is lowered. This phenomenon leads to a considerable departure from a straight-line fit in the conventional plots of $\log G + U^*/2.303R(T - T_\infty)$ against $1/T(\Delta T)$ suggested by nucleation theory. (Here, G is the growth rate, U^* a "universal" constant characteristic of the activation energy of chain motion (reptation) in the melt, R the gas constant, T the crystallization temperature, T_∞ the theoretical temperature at which all motion associated with viscous flow or reptation ceases, $\Delta T = T_m^\circ - T$ the undercooling, and

[†]Dedicated with respect and appreciation to Professor Walter Stockmayer.

[‡]From a dissertation to be submitted to the graduate school, University of Maryland, by E.J.C. in partial fulfillment of the requirements for the Ph.D. degree in Chemical Engineering.

T_m° the melting temperature.) This departure from conventional nucleation theory has not been adequately explained. It is evident that the aforementioned data are much better fitted on such plots by two straight lines than one, which suggests the presence of a regime transition. However, the slope change is in the opposite direction from that predicted for the now familiar regime I \rightarrow regime II transition.¹ A recent development in the kinetic theory of polymer crystallization is the proposal of a regime III in polymer crystallization.² This theory predicts a twofold increase in the slope of plots of $\log G + U^*/2.303R(T - T_\infty)$ vs. $1/T(\Delta T)$ as the crystallization temperature is lowered through the transition point between regime II and regime III. This is equivalent to the prediction of an abrupt upward trend in the growth rate as the crystallization temperature is lowered as one passes from regime II to regime III. In this paper we analyze published i-PP spherulite growth rate data and show that the data are consistent with a regime II \rightarrow regime III transition. We obtain reasonable values for nucleation constants, surface free energies, and the work of chain folding in regimes II and III. Hitherto these same data could not be analyzed (or led to anomalous results) because the regime III theory was not known.

Three regimes of polymer crystallization have been proposed on both theoretical and experimental grounds. Fundamentally, a "regime" transition occurs when the relationship between growth rate and the surface nucleation rate undergoes a change. In the highest temperature regime (denoted "regime I") the observable growth rate, G , varies as i , where i is the surface nucleation rate. Here, one surface nucleus causes completion of a layer of length L on the substrate.¹ In the next lower temperature regime, called "regime II", multiple nucleation occurs on the substrate, and $G \propto i^{1/2}$ (see, for example, ref 1 and 3). This leads to a *downward* break in the growth rate curve as one passes through the regime I \rightarrow regime II transition when the isothermal crystallization temperature is lowered. The presence of a regime I \rightarrow regime II transition has been clearly demonstrated in polyethylene fractions crystallized from the melt,⁴ and it has also been seen in a poly(L-lactic acid) fraction.⁵ At still lower temperatures the mean separation of the nuclei on the substrate approaches the width of the molecular stems, and here regime III is entered; in this regime, $G \propto i$ again, so that at the II \rightarrow III transition there occurs an *upward* break in the growth rate curve.² As shown in recent work,² the regime II \rightarrow regime III transition can be seen in the growth rate data in poly(oxyethylene) and polyethylene.^{2,7} The nucleation rate, i , is a continuous function of the temperature in all three regimes and is controlled by an expression of the form² $\exp[-U^*/R(T - T_\infty)] \exp[-K_g/T(\Delta T)]$, where K_g is the nucleation constant. The quantity i increases rapidly with increasing undercooling ΔT at growth temperatures near the melting point because here the factor $\exp[-K_g/T(\Delta T)]$ is dominant.^{1,2}

Failure to recognize the existence of these three regimes, in which G can be expressed by different powers of i , can lead to an apparent inapplicability of the nucleation theory of spherulite or axialite growth. In somewhat oversimplified terms, the conventional plots of $\log G + U^*/2.303R(T - T_\infty)$ vs. $1/T(\Delta T)$ exhibit considerable curvature near the transitions, which, if their presence were not known or noticed, would frustrate the analysis. Also, quite incorrect values of the fold surface free energy σ_e and the work of chain folding q would be obtained. Actually, the presence of the breaks in the growth rate data is a distinct advantage, since their known properties allow a definite

decision to be made as to which regimes are present, and this in turn permits the data to be analyzed for σ_e and q with confidence.

A number of growth rate studies for i-PP have been published.⁸⁻¹⁸ An abrupt upward curvature in the growth rate data as temperature decreased was distinctly observed by Falkai and Stuart⁸ in 1959, and since then a similar upswing has also been observed in the data of other authors. This upward swing in the growth rate with decreasing temperature is manifested in plots of $\log G + U^*/2.303R(T - T_\infty)$ vs. $1/T(\Delta T)$ as an abrupt increase in slope with decreasing $1/T(\Delta T)$ at a certain value of $1/T(\Delta T)$. (In a later section, we shall identify those data which were taken over a sufficient temperature range to bring out the upswing characteristic of the II \rightarrow III transition.) Although explanations for the upswing in G (usually noticed as a concave-downward curvature in plots of $\log G + U^*/2.303R(T - T_\infty)$ against $1/T(\Delta T)$) have been offered by various authors in the past, none have clearly elucidated the cause of the change in the slope. In this paper we shall show that a regime II \rightarrow regime III transition occurs in the published growth rate data of melt-crystallized i-PP, which addresses directly the central cause of the "curvature" or change of slope noted above. Further, we shall arrive at σ_e and q values for both regimes that are essentially the same, and that are physically reasonable. This clarifies a situation described recently in the literature by Miller and Seeley,¹⁹ wherein it was pointed out (prior to the publication of the theory for regime III) that a strong curvature occurred in i-PP data when the conventional type of plot suggested by nucleation theory was used. They indicated that the presence of this curvature precluded analysis of i-PP data in terms of the then extant theories of growth. The present treatment of i-PP strongly parallels an earlier analysis² of the regime II \rightarrow regime III transition in poly(oxyethylene) (POM) data, which had also been intractable prior to the advent of regime III theory. We shall also draw tentative conclusions regarding the crystallization kinetics of syndiotactic polypropylene (s-PP).

Another feature of the present work is that we shall illustrate a method of obtaining the work of chain folding directly from appropriate plots of the observed growth rate data without the necessity of knowing the enthalpy of fusion. The method, which is useful in all three regimes, is a justifiable simplification based on a simple extension of an earlier treatment.¹

The paper closes with some with some general remarks on the significance of regime III crystallization.

Background

The radial rate of growth, G , of lamellar polymer spherulites or axialites is dependent upon the difference between the crystallization temperature and equilibrium melting temperature appropriate to the chain length under consideration, this difference being denoted as ΔT . The growth rate of polymers during crystallization is then described within a given regime by the equation

$$G = G_0 \exp[-U^*/R(T - T_\infty)] \exp[-K_g/T(\Delta T)] \quad (1)$$

where G_0 is the preexponential factor containing quantities not strongly dependent on temperature. (In regimes I and II, it is permissible to replace $\exp[-U^*/R(T - T_\infty)]$ with $\exp[-Q_D^*/RT]$, where Q_D^* is the measured activation enthalpy of reptation.^{2,20})

The distinction between the three regimes in polymer crystallization is a function of the degree of undercooling and depends on the basic relationship between the nucleation rate i and the overall observable growth rate G at various temperatures.

In regime I, each surface nucleation act quickly causes a new layer of thickness b_0 and length L to be added to the substrate at the growth front before a new nucleation act occurs. As a result, the growth surface of the crystal is essentially smooth for a distance comparable to L because the new substrate layer is complete before a new nucleus forms. In regime I, $G_I \equiv ib_0L$, which leads to^{1,2} $G_I = G_{0(I)} \exp[-U^*/R(T - T_\infty)] \exp[-K_{g(I)}/T(\Delta T)]$ (2a) where

$$K_{g(I)} = 4b_0\sigma\sigma_e T_m^\circ / (\Delta h_f)k \quad (2b)$$

In the above expression for K_g , σ is the lateral surface free energy, σ_e the fold surface free energy, Δh_f the enthalpy of fusion, k Boltzmann's constant, and b_0 the layer thickness. Surface free energies are often quoted in erg cm^{-2} ($1 \text{ mJ m}^{-2} = 1 \text{ erg cm}^{-2}$), and the enthalpy of fusion is given in erg cm^{-3} ($1 \text{ J} = 10^7 \text{ erg}$).

The surface nuclei occur sporadically in time on the substrate at a rate that is dependent upon the temperature and increases as the temperature is lowered. As the degree of undercooling increases, the surface nuclei form more quickly. Regime II commences when the nucleation rate becomes so high that multiple nuclei form on the substrate before the previous layer is complete. The nuclei form at a rate i and each nucleus spawns a substrate completion process that spreads across the surface at a velocity g . The distance between the edges of two adjacent nuclei is termed a "niche distance". The newly formed surface in regime II is uneven and rough on a molecular scale. The growth rate for regime II is given by $G_{II} \equiv b_0(2ig)^{1/2}$, which leads to^{1,2,4}

$$G_{II} = G_{0(II)} \exp[-U^*/R(T - T_\infty)] \exp[-K_{g(II)}/T(\Delta T)] \quad (3a)$$

where

$$K_{g(II)} = 2b_0\sigma\sigma_e T_m^\circ / (\Delta h_f)k \quad (3b)$$

The temperature dependence of G_{II} is almost entirely a result of the factor $i^{1/2}$; g depends on temperature, but much less so than i .

As the undercooling is increased in regime II, the number of surface nuclei per unit length also increases so that the mean distance between adjacent nuclei (i.e., the niche distance) gets smaller. Regime III crystallization begins when the niche distance is reduced to approximately several times the width of a polymer chain stem.² (It has been noted, at least in the case of polyethylene, that the regime II \rightarrow regime III transition is also where steady-state reptation gives way to the reptation of slack²⁰.) Regime III crystallization is accomplished to a considerable extent by primary nucleation of stems on the substrate surface; in the other regimes, almost all of the stems enter the crystal through the substrate completion process. The resulting growth front in regime III is extremely rough on a molecular scale because of the intense multiple nucleation and because more than one growth plane is involved.²¹ The growth rate is proportional to i rather than the square root of i , so that $G_{III} \equiv b_0iL'$, which leads to²

$$G_{III} = G_{0(III)} \exp[-U^*/R(T - T_\infty)] \exp[-K_{g(III)}/T(\Delta T)] \quad (4a)$$

where

$$K_{g(III)} = 4b_0\sigma\sigma_e T_m^\circ / (\Delta h_f)k \quad (4b)$$

In the above, L' is the effective substrate length,² which corresponds to $\sim(2-3)a_0$, where a_0 is the width of the chain stem. In general, L' is considerably smaller than L .

Regime I crystallization prevails at high temperatures, closest to the melting point where the growth rates are the

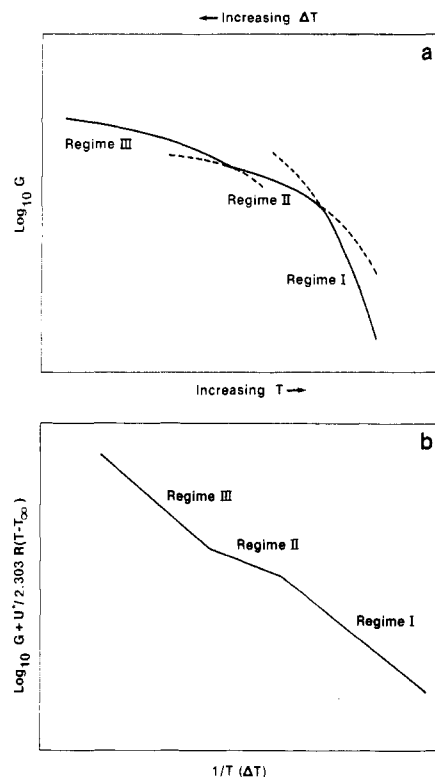


Figure 1. Typical growth rate curves for a lamellar polymer illustrating regimes I, II, and III. (Schematic after ref 2.)

slowest. Regime III crystallization takes place at large undercoolings where growth rates are most rapid. Regime II occurs in the intermediate region. The transition between regimes occurs at different temperatures and degrees of undercooling for various polymers. In general, there is a maximum in $G(T)$ as a function of crystallization temperature at roughly $(0.7-0.8)T_m^\circ$. In some cases, regime III may occur below the maximum where the factor $\exp[-U^*/R(T - T_\infty)]$ is dominant and thus be masked. In the polymer to be discussed here, the II \rightarrow III transition occurs well above the maximum in $G(T)$ and is therefore readily observable.

Figure 1 depicts typical polymer growth rate curves schematically illustrating the location of regimes I, II, and III. In Figure 1a, $\log G$ (cm s^{-1}) is plotted as a function of temperature and undercooling. Location of the three regimes is indicated. Within a given regime the growth rate of polymers is represented by eq 1. Taking the log of eq 1, one obtains

$$\log G = \log G_0 - U^*/2.303R(T - T_\infty) - K_g/2.303T(\Delta T) \quad (5)$$

The overall picture of regime crystallization is best shown by plots of $\log G + U^*/2.303R(T - T_\infty)$ against $1/T(\Delta T)$. Such a plot is illustrated schematically in Figure 1b. The transitions between the regimes are distinctly shown by changes in the slope, and if a break is seen, it is immediately apparent which two regimes are involved. It is evident that growth rates in regime III are greater than would be predicted at the same undercooling with regime II theory.

Values for K_g and G_0 can be obtained directly from the graph, where the slope is $-K_g/2.303$ and the intercept is equal to $\log G_0$. Once K_g is known, other parameters characteristic of crystal growth can be determined. From the above it can be seen that the nucleation constant K_g for regimes I and III is the same, which is illustrated in Figure 1b, where the slopes for regimes I and III are shown

as equal. Also, the nucleation constant for regimes I and III is twice that for regime II; i.e., $K_{g(I)} = K_{g(III)} = 2K_{g(II)}$. The preexponential factor, G_0 , for regime III is substantially less² than that for regime I, since $G_{0(I)}/G_{0(III)} = L/L'$. In the case of polyethylene, L is estimated to be $\sim 0.11 \mu\text{m}$,^{2,20} so that with $L' \sim 2a_0 = 9.10 \text{ \AA}$ one finds $G_{0(I)}/G_{0(III)} \sim 120$.

Below we outline two convenient methods of analyzing the growth rate data. One assumes that the heat of fusion is known and yields both σ and σ_e quite directly. The second method, actually algebraically identical with the first, deals in an expeditious manner with cases where the heat of fusion is not known and gives only σ_e . In both approaches, the calculation of the crystal growth parameters rests on knowledge of a_0 , the width of the chain stem, and b_0 , the thickness of the molecular layer added, which provide the cross-sectional area of the chain a_0b_0 . They are derived from the unit cell parameters and the crystal growth plane.

The first approach may be used when Δh_f is known. A value for σ is estimated from Δh_f by¹

$$\sigma = \alpha \Delta h_f (a_0 b_0)^{1/2} \quad (6)$$

where $\alpha \simeq 0.1$. This σ is applicable in all regimes. Then $\sigma\sigma_e$ can be obtained by rearrangement of eq 3b and 4b, which leads to

$$\sigma\sigma_e = K_{g(II)} \Delta h_f k / (2b_0 T_m^\circ) \quad (7)$$

for regime II and

$$\sigma\sigma_e = K_{g(III)} \Delta h_f k / (4b_0 T_m^\circ) \quad (8)$$

for regime III. Here it is understood that $K_{g(II)}$ and $K_{g(III)}$ are experimentally determined values. The corresponding values of σ_e are obtained by dividing $\sigma\sigma_e$ values by σ from eq 6:

$$\sigma_e = \sigma\sigma_e / \sigma \quad (9)$$

The principal contribution to the fold surface free energy is the work of chain folding required to bend the polymer chain back upon itself so that it can reenter the crystal in a manner consistent with the lattice structure. The work of chain folding is derived from the fold surface free energy by

$$q = 2\sigma_e a_0 b_0 \quad (10)$$

where, as noted earlier, a_0b_0 represents the cross-sectional area of the polymer chain.

When the heat of fusion is not known, a second approach must be used. The heat of fusion is eliminated from eq 3b and 4b by substitution of σ from eq 6. Then rearrangement yields

$$\sigma_e = K_{g(II)} k / [2b_0 T_m^\circ \alpha (a_0 b_0)^{1/2}] \quad (11)$$

for regime II and

$$\sigma_e = K_{g(III)} k / [4b_0 T_m^\circ \alpha (a_0 b_0)^{1/2}] \quad (12)$$

for regimes I and III. Using eq 10 it follows that the work of chain folding in regime II can be estimated directly from an experimental $K_{g(II)}$ by

$$q = a_0 K_{g(II)} k / [T_m^\circ \alpha (a_0 b_0)^{1/2}] \quad (13)$$

and likewise in regime III

$$q = a_0 K_{g(III)} k / [2T_m^\circ \alpha (a_0 b_0)^{1/2}] \quad (14)$$

With this second approach, σ_e and q can be found, but no value for σ is obtained since it is a function of the enthalpy of fusion as is seen in eq 6.

Analysis

A number of sets of growth rate data for monoclinic i-PP spherulites were taken from the literature for reanalysis

Table I
Values of Isotactic Polypropylene Material Constants

crystal chain conformation ^a	3, helix
T_m° , ^b °C	185
T_g° , ^c °C	-12
Δh_f , ^d J/g	209.3 ± 29.9^e
ρ , ^f g/cm ³	0.936^e
unit cell parameters ^a	
a , Å	6.65
b , Å	20.96
c , Å	6.50
β , deg	99.3
(110) growth plane	
a_0 , Å	5.49
b_0 , Å	6.26
$a_0 b_0$, Å ²	34.37
(040) growth plane	
a_0 , Å	6.56
b_0 , Å	5.24
$a_0 b_0$, Å ²	34.37

^a Reference 24. ^b Reference 23. ^c Reference 25.

^d Reference 22. ^e Combination of these values gives $\Delta h_f = 1.96 \times 10^9 \text{ erg cm}^{-3}$. ^f Reference 26.

in this paper. The i-PP material constants used in this analysis were selected after evaluation of data in the literature and are listed in Table I. The literature contains a number of conflicting values for the melting temperature, glass transition temperature, heat of fusion, and density. The glass transition temperature is needed so that T_∞ can be estimated. The melting temperature is usually the most critical in this type of analysis. Krigbaum²² has determined the melting temperature of monoclinic i-PP to be $186 \pm 2^\circ\text{C}$, while Samuels²³ has found it to be 185°C , and Miller¹⁹ has used 186°C . A value of $T_m^\circ = 185^\circ\text{C}$ was used here. The effect of $\pm 1^\circ\text{C}$ melting temperature change on q and σ_e is relatively small in this case because of the large undercooling involved and will be noted subsequently. The sensitivity of q , σ_e , and σ to changes in T_g , Δh_f , and ρ was also evaluated. Table I lists the values for the i-PP crystalline chain conformation,²⁴ melting temperature,²³ glass transition temperature,²⁵ enthalpy of fusion,²² density,²⁶ and unit cell parameters²⁴ used in this paper.

Determination of K_g for i-PP. The i-PP growth rate data of Binsbergen and deLange,¹⁴ Falkai and Stuart,^{8,9} and Goldfarb¹⁶ span a wide enough temperature range to clearly show the regime II \rightarrow regime III transition. These three data sets are plotted in Figure 2 for $U^* = 1500 \text{ cal/mol}$ ($1 \text{ cal} = 4.184 \text{ J}$), and $T_\infty = T_g - 30^\circ\text{C} = 231.2 \text{ K}$, and $T_m^\circ = 185^\circ\text{C} = 458.2 \text{ K}$. An upward change of slope is clearly evident in each of the three data sets. It is immediately seen that an attempt to put one straight line through all the data would lead to an inadmissible fit. Two straight lines were fitted to each data set, one line to the data judged to be above the transition temperature and the second to the data below the transition. The data at temperatures below the slope change on the $1/T(\Delta T)$ scale are in regime III and those at temperatures above it correspond to regime II. The transition occurs near 137°C . The lines through the three sets of data within a given regime are essentially parallel. (The reason for the vertical offset among the lines is likely a difference in molecular weight or tacticity of the polymers; a high molecular weight tends to give a slower crystallization rate at a given undercooling.²) The slope of each line was calculated, and values of K_g in regimes II and III were obtained for each set. Under the numerical headings 1–3, Table II lists the values for slope, K_g , and correlation coefficients for the data depicted in Figure 2. The K_g values for each regime are similar for the three sets of data, and the ratios of

Table II
Slope, Nucleation Constants, and Correlation Coefficients for Isotactic Polypropylene Growth Rate Data in Regimes II and III for the Case $U^* = 1500$ cal/mol, $T_\infty = 231.2$ K, and $T_m^0 = 458.2$ K

data source	slope $\times 10^{-4}$ in deg ²	$K_g \times 10^{-5}$ in deg ²	G_0 , cm/s	no. of data points	corr coeff	$K_{g(III)}/K_{g(II)}$
Regime II						
1. Binsbergen and deLange ¹⁴	-6.585 ± 0.52	1.516	0.3048	5	0.9909	2.383
2. Falkai and Stuart ^{8,9}	-6.943 ± 0.53	1.599	0.3573	3	0.9972	1.991
3. Goldfarb ¹⁶	-7.110	1.637	0.8802	2		1.991
		1.584 ^a	0.5141 ^a			2.087 ^b
Regime III						
1. Binsbergen and deLange ¹⁴	-15.69 ± 0.19	3.613	9683	4	0.9999	
2. Falkai and Stuart ^{8,9}	-13.82 ± 0.38	3.183	1059	6	0.9985	
3. Goldfarb ¹⁶	-14.16 ± 0.38	3.260	3516	6	0.9986	
4. Keith and Padden ¹³	-14.52 ± 0.31	3.344	2427	4	0.9995	
5. Lovinger, Chua, and Gryte ¹⁵	-14.22 ± 0.41	3.274	1778	11	0.9963	
6. Martuscelli, Sylvester, and Abate ¹⁸	-15.56 ± 0.34	3.584	8009	9	0.9983	
7. Wlochowicz and Eder ¹⁷	-13.55 ± 0.26	3.121	1400	10	0.9986	
		3.340 ^a	3990 ^a			

^a Average values. ^b K_g values used in calculating this ratio are from the three data sets having both regime II and regime III data (items 1-3 above).

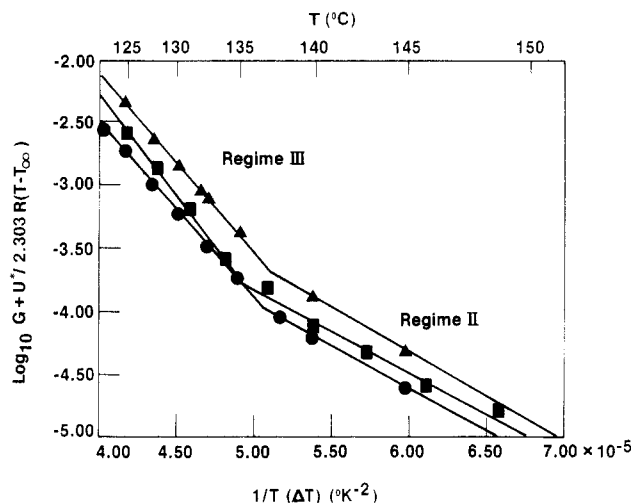


Figure 2. Plot of $\log G + U^*/2.303R(T - T_\infty)$ against $1/T(\Delta T)$ for i-PP in regimes II and III for the case $U^* = 1500$ cal/mol, $T_\infty = T_g - 30^\circ\text{C} = 231.2$ K, and $T_m^0 = 458.2$ K, where G is in cm s⁻¹; (●) data of Falkai and Stuart;⁸ (▲) data of Binsbergen and deLange;¹⁴ (▲) data of Goldfarb.¹⁶

$K_{g(III)}/K_{g(II)}$ are near 2, which is the value predicted by theory. If the value of U^* is reduced to zero, the values of K_g are reduced about 12% but the ratio of $K_{g(III)}/K_{g(II)}$ remains essentially unchanged. Thus, in the range of the present data, the temperature dependence of G is almost entirely in the K_g term in eq 1, the factor $\exp[-U^*/R(T - T_\infty)]$ behaving as a relatively unimportant correction term. At sufficiently low temperatures, the latter factor would dominate $G(T)$, but this is not relevant to the present study.

Four additional sets of i-PP growth rate data were also analyzed in regime III. The data of Keith and Padden¹³ and Lovinger, Chua, and Gryte¹⁵ are in regime III but did not extend into the temperature range of regime II. Lovinger and Gryte's data for α -type crystals were used. Martuscelli, Sylvester, and Abate's data¹⁸ did not go high enough into the temperature range of regime II to clearly define the transition. However, their two data points above

the apparent transition temperature suggest the possibility of a break in their data also. The data of Wlochowicz and Eder¹⁷ extend into the temperature range for regime II but show anomalous behavior in the regime II region. Thus the last four data sets were analyzed only in terms of regime III. Values for the regime III slope, K_g , and the corresponding calculated correlation coefficients for these four data sets are also shown in Table II. The values are similar to the corresponding values calculated from the earlier three data sets and confirm the regime III results.

It is interesting to note that the sign of the birefringence of i-PP spherulites changes near the II \rightarrow III transition.¹¹

Determination of σ , σ_e , and q for i-PP. With K_g known, the surface free energies and the work of chain folding can be calculated. First, σ , σ_e , and q will be calculated by using the enthalpy of fusion and other material constants listed in Table I. Assuming crystal growth on the (110) plane, a value of $\sigma = 11.5$ erg/cm² is obtained from eq 6 when $\alpha = 0.1$. Using the K_g values from Table II and eq 7-10, we calculated σ_e , σ , and q for regimes II and III (see Table III). The data in Table III indicate the fold surface free energy and the work of chain folding are close to the same in both regimes II and III. Values of $\sigma_e = 740-790$ erg²/cm⁴, $\sigma = 65-70$ erg/cm², and $q = 6.4-6.8$ kcal/mol folds are found. These are reasonable and consistent with values of other polymers. If $U^* = 0$, all values are about 12% lower. The values calculated with $U^* = 1500$ cal mol⁻¹ are of course to be preferred.

Some error is undoubtedly incurred by assuming growth only on the (110) plane, since it is now known from the theoretical work of Guttman and DiMarzio²¹ that growth on more than one lattice plane must occur in regime III. This is a physical requirement for regime III growth. However, the fact that the experimental value of $K_{g(III)}$ is very nearly exactly twice that of $K_{g(II)}$ implies that the error is small.

The quantities σ_e and q can also be calculated without using Δh_f . Equations 11-14 with $\alpha = 0.1$ are used to accomplish this. The σ_e and q obtained are necessarily identical with those determined previously. In the first approach, Δh_f was used to determine both σ_e and σ ;

Table III
Surface Free Energy and Work of Chain Folding for
Isotactic Polypropylene^a

data source	$\sigma\sigma_e$, erg ² /cm ⁴	σ_e , erg/cm ²	q , kcal/ (mol of folds)
Regime II			
1. Binsbergen and deLange ¹⁴	714.2	62.3	6.159
2. Falkai and Stuart ^{8,9}	753.1	65.7	6.494
3. Goldfarb ¹⁶	771.1	67.2	6.650
	746.1 ^b	65.1 ^b	6.434 ^b
Regime III			
1. Binsbergen and deLange	850.8	74.2	7.336
2. Falkai and Stuart	749.6	65.4	6.464
3. Goldfarb	767.7	66.9	6.620
4. Keith and Padden ¹³	787.4	68.7	6.790
5. Lovinger, Chua, and Gryte ¹⁵	770.9	67.2	6.648
6. Martuscelli, Sylvestre, and Abate ¹⁸	843.9	73.6	7.278
7. Wlochowicz and Eder ¹⁷	735.0	64.1	6.338
	786.5 ^b	68.6 ^b	6.782 ^b

^a Calculated for the case $U^* = 1500$ cal/mol, $T_\infty = 231.2$ K, $T_m^\circ = 458.2$ K, $\sigma = 11.5$ erg cm⁻², and (110) growth plane. ^b Average values.

consequently, in the algebraic cancellation involved in eq 9 when $\sigma\sigma_e$ was divided by σ to get σ_e , the effect of Δh_f was eliminated. Thus both approaches provide the same result in calculating σ_e and q ; however, σ can be estimated only when Δh_f is known.

Estimate of G_0 for i-PP. The preexponential factor G_0 is obtained from plots of $\log G + U^*/2.303R(T - T_\infty)$ vs. $1/T(\Delta T)$, where the intercept is $\log G_0$. Table II lists the G_0 values estimated for regimes II and III. Using the theory for $G_{0(III)}/G_{0(II)}$ given in ref 2, which shows that the dominant factor in determining this quantity is $\exp(-q/2kT)$, with the same parameters as POM, but using $q = 6.6$ kcal/mol in the case of i-PP, we find the theoretical value to be 3.6×10^4 . The measured value is 3×10^3 to 3×10^4 for the data sets showing both regimes.

The growth rate of i-PP will be exceedingly slow in regime I, as can be seen qualitatively in comparing Figures 1b and 2. This evidently accounts for the fact that there are no growth rate measurements for i-PP in the literature at the high temperatures that are required to permit regime I kinetics. Accordingly, experimental values of $G_{0(I)}$ are not currently available for comparison with $G_{0(II)}$ and $G_{0(III)}$. If regime I could be found for i-PP and a value of G_0 obtained, one could estimate L from the ratio $G_{0(II)}/G_{0(III)} = L/L'$ since L' is known to be $\sim 2a_0$ to $3a_0$. Thus it would be well worth the effort to locate regime I in this polymer. This paper has dealt solely with the α -form of i-PP. Clearly, it would be of interest to examine the question of regime transitions in the β -form as well. Some data on

the β -form are known¹⁵ but would have to be extended in temperature range in order to locate the transition.

Effect of Change in Material Properties. The effect of changing values of the constants for i-PP in Table I was evaluated. A 1 °C change in T_m° causes approximately a 5% change in K_g , σ_e , and q . K_g values are relatively insensitive to changes in T_g . Variation in the melting temperature or growth plane does not affect σ . However, changes in Δh_f and ρ affect σ but not σ_e or q . When Δh_f is varied by 0.3×10^9 erg/g, σ changes about 14%, while a variation of 0.01 in α results in a 10% change in σ , σ_e , and q . A 0.01 g/cm³ alteration of ρ has only about a 1% effect on σ . Choice of different growth planes affects σ_e and q . A 20% increase occurs if all crystal growth is assumed to take place on the (040) plane. A recent discussion of some possible growth planes in i-PP has been given by Lovinger.²⁷ As we noted earlier, "mixed" growth planes must occur in regime III.

Syndiotactic Polypropylene. We have examined the syndiotactic polypropylene (s-PP) growth rate data of Miller and Seeley.¹⁹ In plots similar to Figure 2 using $T_m^\circ = 161$ °C (434.2 K), the bulk of the data fit a straight line above temperatures corresponding to $\Delta T \sim 50$ °C. It appears by their general position on a $\log G + U^*/2.303R(T - T_\infty)$ vs. $1/T(\Delta T)$ plot that these data are in regime II, where we estimate $\sigma_e = 49.9$ erg/cm² and $q = 5.8$ kcal/mol of folds. At an undercooling $\Delta T \sim 50$ °C, there is a possible break. Because of a lack of data below 115 °C, where we suspect the break, confirmation of regime III is not possible with these data. Further experimental work might disclose a regime II \rightarrow regime III transition in s-PP at about 110–115 °C; careful experiments at small temperature increments would be necessary to show whether or not the transition exists in s-PP.

Comparison of i-PP and s-PP with Other -C-C- Backbone Hydrocarbon Polymers. The values of σ , σ_e , and q found in this analysis are compared with other -C-C- backbone hydrocarbon polymers in Table IV. Each of these polymers has a carbon-carbon backbone but different side groups. The side groups make the chain stiffer, resulting in a higher melting temperature. As the melting temperature rises, the work of chain folding increases because the stiffer chain is harder to bend to make the fold. Thus one would expect q to increase as T_m° increases. Observe that it is q , and not σ_e , that scales smoothly upward as T_m° increases. This point has been made previously,¹ but Table IV gives a more complete illustration of this than was heretofore available.

Summary, Conclusions, and General Significance of Regime III

Recognition of the existence of the regime II \rightarrow regime III transition permits analysis of polymer growth rate data in the literature where previous analysis using conventional nucleation theory had failed to explain the data. In the present analysis, growth rate data for i-PP and s-PP have been plotted in a manner designed to disclose the presence

Table IV
Comparison of Surface Free Energies and Work of Chain Folding for Polypropylene and Other -C-C- Backbone Polymers

	T_m° , °C	regime	σ , erg/cm ²	σ_e , erg/cm ²	q , kcal/ (mol of folds)	source
poly(1-butene) (form 2)	128	II	7.2	30.8 ^a	4.9	ref 28
polyethylene	145	I, II, III	11.1–14.1	93.8	5.3–5.7	ref 1 and 20
syndiotactic polypropylene	161	II		~ 49.9	~ 5.8	this work
isotactic polypropylene	185	II, III	11.5	65–70	6.4–6.8	this work
isotactic polystyrene	242	II	7.64	35	7.1	ref 29

^a Calculated for regime II. This doubles the $\sigma\sigma_e$ and q values given in ref 28.

of regime transitions. On a plot of $\log G + U^*/2.303R(T - T_\infty)$ vs. $1/T(\Delta T)$, a regime II \rightarrow regime III transition is evidenced by a distinct upward change of the slope as the temperature is decreased. Analysis of the slope data permits estimates to be made for K_g , q , and σ_e for comparison with values for other polymers.

Clear evidence of a regime II \rightarrow regime III transition was found in the i-PP data: an upward slope change typical of a regime II \rightarrow regime III transition was found at approximately 137 °C ($\Delta T \sim 48$ °C). Analysis of the nucleation constant data yielded 2.087 for the ratio of $K_{g(\text{III})}/K_{g(\text{II})}$ for i-PP, which is in good agreement with the theoretical value of 2. Both q and σ_e were estimated for i-PP from the K_g values and found to be approximately the same for both regimes, as they should be. The values of $q = 6.4\text{--}6.8$ kcal/mol of folds and $\sigma_e = 65\text{--}70$ erg/cm² estimated for i-PP are reasonable and fit into the range of values for other polymers. The lateral surface free energy was also estimated from the enthalpy of fusion data for i-PP and found to be $\sigma = 11.5$ erg/cm², which is reasonable.

The s-PP data did not show a clear regime II \rightarrow regime III transition, but this may well have been because growth rate data over a sufficiently broad temperature range are lacking. The available s-PP data have the general character of regime II data. When we assumed most data were in regime II, we estimated $\sigma_e = 49.9$ erg/cm² and $q = 5.8$ kcal/mol of folds, which are reasonable values consistent with the crystal structure and compare favorably with other hydrocarbon polymers.

The work of chain folding for i-PP, s-PP, polyethylene, and other hydrocarbon polymers fall into a sequence indicating q increases as T_m° increases.

Having established a reasonable case for the manifestation of regime III growth in i-PP, and recalling that it has been observed in polyethylene and poly(oxy-methylene), we close this paper by noting its general scientific and technological significance.

The sharp upswing in growth rate with decreasing temperature that occurs when regime III is entered has technological importance because rapidly cooled specimens of appropriately small dimensions are apt to crystallize in this regime; except for very thin specimens, the heat of fusion liberated during the rapid growth would tend to confine the crystallization to the higher temperature portion of regime III even when the specimen is quenched. This and associated points have been discussed by Keith and Loomis³⁰ for polyethylene in a manner suitable for dealing with both scientific and technological applications. Many polymeric objects made by quenching the polymers mentioned may contain considerable material with the molecular morphology characteristic of regime III. This morphology has features that are important in determining properties.

In remarking on the molecular morphology in regime III, we use polyethylene as a guide. We would expect the chain morphology of quench-crystallized i-PP (i.e., regime III i-PP) to be generally similar in character. It has been shown elsewhere that the "variable-cluster" model² is appropriate in regime III. In this model the adjacent or very nearly adjacent chain folding occurs in small clusters involving two to three stems. The clusters are connected together by chains with amorphous character that are either interlamellar links ("tie" molecules) between two different lamellae or nonadjacent reentries, where the chain reenters the same lamella at a distant site ("loops"). The tie molecules and nonadjacent events comprise the amorphous phase in the semicrystalline system. It is im-

portant to note that well over half of the crystalline stems involve "tight" folds, i.e., folds where reentry is either strictly adjacent or very nearly adjacent. If there were less "tight" folding than this, a serious density paradox would occur at the lamellar surface.^{2,31} Thus the surfaces of the lamellae may reasonably be described as mostly chain folded, but with "mistakes" in the ideal folding process that manifest themselves as loops and tie molecules. The "tight" folds make no contribution to the amorphous phase. The variable-cluster model has the interesting property of exhibiting a high degree of adjacency or very near adjacency together with a radius of gyration that varies as $M^{1/2}$. The tie molecules occupy roughly 5–10% of the surface sites. These must play a role in toughening the polymer.

It has recently been shown that regime III can occur only when more than one growth plane is involved.²¹ Thus one must expect to find chain-folded clusters in more than one growth plane. This result is general for regime III and applies to i-PP. In the analysis of neutron scattering data for polymers crystallized in regime III, this has importance since some of the planes will involve stems with a larger than usual separation, which will reduce the scattering intensity at intermediate angles. Also, the fold surface disorder will tend to be maximized in regime III.² Failure to appreciate these points can in the first instance lead to an underestimate of the degree of adjacency or very near adjacency in the analysis of neutron scattering experiments, and in the second to unduly sweeping conclusions that inadvertently ascribe the chain morphology with maximal disorder appropriate only to regime III to higher temperature regimes where larger chain-folded clusters may form.

We have already noted that the observation of regime transitions permits a relatively certain assignment of the specific regimes involved, with the result that reasonably accurate σ_e and q values can be obtained. Finally, we observe that the existence of regime III crystallization in polymers invites a parallel inquiry with regard to the possibility of a phenomenon of similar character in other types of materials.

Registry No. Isotactic polypropylene (homopolymer), 25085-53-4; syndiotactic polypropylene (homopolymer), 26063-22-9.

References and Notes

- Hoffman, J. D.; Davis, G. T.; Lauritzen, J. I., Jr. In "Treatise on Solid State Chemistry"; Hannay, N. B., Ed.; Plenum Press: New York, 1976; Vol. 3, Chapter 7.
- Hoffman, J. D. *Polymer* **1983**, *24*, 3.
- Sanchez, I. C.; DiMarzio, E. A. *J. Res. Natl. Bur. Stand., Sect. A* **1972**, *76*, 213–223.
- Hoffman, J. D.; Frolen, L. J.; Ross, G. S.; Lauritzen, J. I., Jr. *J. Res. Natl. Bur. Stand., Sect. A* **1975**, *79*, 671.
- Vasanthakumari, R.; Pennings, A. J. *Polymer* **1983**, *24*, 175.
- Pelzbauer, Z.; Galeski, A. *J. Polym. Sci., Part C* **1972**, *38*, 23.
- Barham, P. J.; Jarvis, D. A.; Keller, A. J. *J. Polym. Sci., Polym. Phys. Ed.* **1982**, *20*, 1733.
- Falkai, B. V.; Stuart, H. A. *Kolloid Z.* **1959**, *162*, 138.
- Falkai, B. V.; Stuart, H. A. *Makromol. Chem.* **1960**, *41*, 86.
- Marker, L.; Hay, P. M.; Tilley, G. P.; Early, R. M.; Sweeting, O. J. *J. Polym. Sci.* **1959**, *38*, 33.
- Padden, F. J., Jr.; Keith, H. D. *J. Appl. Phys.* **1959**, *30*, 1479.
- Limbert, F. J.; Baer, E. *J. Polym. Sci., Part A* **1963**, *1*, 3317.
- Keith, H. D.; Padden, F. J., Jr. *J. Appl. Phys.* **1964**, *35*, 1286.
- Binsbergen, F. L.; deLange, B. G. M. *Polymer* **1970**, *11*, 309.
- Lovinger, A. J.; Chua, J. O.; Gryte, C. C. *J. Polym. Sci., Polym. Phys. Ed.* **1977**, *15*, 641.
- Goldfarb, L. *Makromol. Chem.* **1978**, *179*, 2297.
- Wlochowicz, A.; Eder, M. *Polymer* **1981**, *22*, 1285.
- Martuscelli, E.; Silvestre, C.; Abate, G. *Polymer* **1982**, *23*, 229.
- Miller, R. L.; Seeley, E. G. *J. Polym. Sci., Polym. Phys. Ed.* **1982**, *20*, 2297.
- Hoffman, J. D. *Polymer* **1982**, *23*, 656.

- (21) Guttman, C. M.; DiMarzio, E. A. *J. Appl. Phys.* **1983**, *54*, 5541.
 (22) Krigbaum, W. R.; Uematsu, I. *J. Polym. Sci., Part A* **1965**, *3*, 767.
 (23) Samuels, R. J. *J. Polym. Sci., Polym. Phys. Ed.* **1975**, *13*, 1417.
 (24) Natta, G.; Corradini, P. *Nuovo Cimento* **1960**, *15* (Suppl. No. 1), 9.
 (25) Jarrigeon, M.; Chabert, B.; Chatain, D.; Lacabanne, C.; Nemoz, G. *J. Macromol. Sci., Phys.* **1980**, *B17*, 1.
 (26) Natta, G. *J. Polym. Sci.* **1955**, *16*, 143.
 (27) Lovinger, A. J. *J. Polym. Sci., Polym. Phys. Ed.* **1983**, *21*, 97.
 (28) Powers, J.; Hoffman, J. D.; Weeks, J. J.; Quinn, F. A., Jr. *J. Res. Natl. Bur. Stand., Sect. A*, **1965**, *69*, 335.
 (29) Lauritzen, J. I., Jr.; Hoffman, J. D. *J. Appl. Phys.* **1973**, *44*, 4340.
 (30) Keith, H. D.; Loomis, T. C. *J. Polym. Sci., Polym. Phys. Ed.* **1984**, *22*, 295.
 (31) Guttman, C. M.; DiMarzio, E. A.; Hoffman, J. D. *Polymer* **1981**, *22*, 1466.

Hypersonic Attenuation in Poly(dimethylsiloxane) as a Function of Temperature and Pressure

Gary D. Patterson,* Patrick J. Carroll, James R. Stevens,[†] William Wilson,[‡] and Harvey E. Bair

AT&T Bell Laboratories, Murray Hill, New Jersey 07974. Received July 20, 1983

ABSTRACT: Hypersonic relaxation is studied in amorphous poly(dimethylsiloxane) (PDMS) as a function of temperature from 77 to 300 K and as a function of pressure at 296 K. A clear loss maximum as a function of pressure was found at 296 K. The loss maximum at 1 bar was found to be at 218 K at a frequency of 5.4 GHz. This is well below the melting point of PDMS (230 K), and the samples had to be carefully supercooled. Successful spectra were obtained down to 200 K. Shock-quenched amorphous samples could be studied up to 157 K. The present results were combined with dielectric relaxation studies of PDMS at 298 K and very high frequencies (159 GHz) and on shock-quenched samples at lower frequencies in the range of 150–160 K to calculate the empirical WLF parameters at the glass transition (146 K). The results were $c_1^g = 14.6$ and $c_2^g = 20$ K. This led to a fractional free volume at T_g of 0.030, which is quite normal. Previous WLF parameters for PDMS were based on an invalid extrapolation of viscosity data obtained above the melting point, where the local relaxation frequencies exceed 10 GHz. The present results place PDMS back within the normal range for polymers.

1. Introduction

Poly(dimethylsiloxane) (PDMS) has one of the lowest glass transition temperatures of all polymers¹ ($T_g \approx 146$ K). This corresponds to the temperature at which the volume or enthalpy relaxation time is near 10 s. Brillouin spectroscopy measures the velocity and attenuation of hypersonic (GHz) acoustic phonons. Light is scattered by thermal sound waves and the basic experiment consists of measuring the spectrum of the scattered light. A typical Rayleigh-Brillouin spectrum is shown in Figure 1. It consists of a central Rayleigh peak and two shifted Brillouin peaks with splitting $\Delta\omega_1$ and line width Γ_1 . The longitudinal Brillouin splitting (frequency) is given by

$$\Delta\omega_1 = qV_1(q) \quad (1)$$

where $q = (4\pi n/\lambda) \sin(\theta/2)$ is the magnitude of the scattering vector, n is the refractive index, λ is the wavelength of the incident light in a vacuum, θ is the scattering angle in the scattering plane, and $V_1(q)$ is the longitudinal velocity for phonons of wave vector magnitude q . The longitudinal Brillouin line width is given by

$$\Gamma_1 = \alpha V_1(q) \quad (2)$$

where α is the attenuation coefficient. Hypersonic attenuation is also expressed in terms of the loss tangent

$$\tan \delta = 2\Gamma_1/\Delta\omega_1 \quad (3)$$

When the local structural relaxation times are in the same range as the inverse Brillouin frequency, the hypersonic attenuation exhibits a maximum. Since the frequencies

are so high (4–10 GHz), the temperature range in which the average relaxation time is comparable to the inverse Brillouin frequency is well above the usual glass transition. The temperature at which the hypersonic attenuation reaches a maximum at 1 bar is typically² 150–200 K above T_g . Thus, even for PDMS the hypersonic loss maximum might be expected to be near room temperature. The earliest study of PDMS by Brillouin spectroscopy³ examined the hypersonic attenuation in the temperature range 273–373 K. No clear indication of a hypersonic loss maximum was observed in this range, and the Brillouin frequency remained lower than that usually associated with such a maximum (5–6 GHz). Measurements were extended to lower temperatures by Lindsay et al.,⁴ but the precision of the results was limited. The lower limit was 220 K and an apparent maximum was reported at 230 K. However, PDMS is a crystallizable polymer and its melting point is 230 K. There is evidence that the sample was partially crystalline below this temperature⁴ since the sound velocity showed a jump at the melting point. We can now obtain high-precision Rayleigh-Brillouin spectra at temperatures from 4 to 600 K. We can also measure the spectrum as a function of pressure. In the present paper we report the measurement of the Rayleigh-Brillouin spectrum of two molecular weight samples of PDMS as a function of temperature from 77 to 300 K and as a function of pressure at 296 K. The results are then discussed in terms of the full frequency dependence of the glass-rubber relaxation and compared to other measurements of viscoelasticity in PDMS.

2. Theory

The phenomenological theory of Rytov⁵ provides a complete framework for the description of Rayleigh-Brillouin scattering in amorphous liquids and solids. The

* Department of Physics, University of Guelph, Guelph, Ontario, Canada N1G 2W1.

[†] Department of Chemistry, Stanford University, Stanford, California 94305.